Colloid Polym Sci (2015) 293:3213–3224
DOI 10.1007/s00396-015-3746-x

INVITED ARTICLE

Ionic-liquid-based surfactants with unsaturated head group: synthesis and micellar properties of 1-(n-alkyl) -3-vinylimidazolium bromides

Naved I. Malek[1,2] · **Zuber S. Vaid**[1] · **Utkarsh U. More**[1] · **Omar A. El Seoud**[2]

Received: 1 July 2015 / Revised: 13 August 2015 / Accepted: 14 August 2015 / Published online: 2 September 2015
© Springer-Verlag Berlin Heidelberg 2015

Abstract Structural versatility is an important reason for the interest in ionic liquids (ILs) and ionic-liquid-based surfactants, ILBSs. We report here on the synthesis, characterization, and micellar properties of a series of ILBSs that carry unsaturation in the head group, 1-C_n-3-vinlyimidazolium bromide, C_nVnImBr, C_n = C_{10}, C_{12}, C_{14}, and C_{16}, respectively. We studied this series at 298.15 K using surface tension, ultraviolet–visible (UV–vis) spectroscopy, and steady state fluorescence of solubilized methyl orange, MO, and pyrene, respectively. We studied the electrical conductance of C_nVnImBr at 298.15 to 313.15 K. From the results of surface tension and conductivity, we calculated the area per surfactant at solution/air interface; the critical micelle concentration (cmc); the degree of counter-ion binding; and the enthalpy, entropy, and free energy of micellization. These properties showed the expected dependence on the length of C_n, and indicated that micellization is an entropy-driven process. We used fluorescence data to calculate the cmc, microscopic polarity of the interfacial region, and the micelle aggregation number. The UV–vis spectra of MO were used to calculate the cmc and probe dye–ILBS interactions in the pre- and post-micellar regimes. The aggregation behavior of C_{16}VnImBr was compared with its saturated counterpart 1-(n-hexadecyl)-3-ethylimidazolium bromide, with 1-C_n-3-methylimidazolium bromides, and with "conventional" cationic surfactants, alkyltrimethylammonium bromides. The vinyl group is less hydrophobic than the ethyl moiety.

Keywords Ionic-liquid-based surfactants, aggregation of · 1-Alkyl-3-vinylimidazolium bromides, micellar properties of · Cationic micelles, properties of · Thermodynamic parameters of micellization · Micelle-solubilized probes

Abbreviations

A_{min}	Area per surfactant molecule at air–water interface
db	Double bond
cmc	Critical micelle concentration
CPC	1-Cetylpyridinium chloride
C_nVnImBr	1-(n-Alkyl)-3-vinylimidazolium bromide
C_{16}EtImBr	1-(n-Hexadecyl)-3-ethylimidazolium bromide
C_nMeImBr	1-(n-Alkyl)-3-methylimidazolium bromide
C_nMe_3ABr	N-(n-Alkyl)-N,N,N-trimethylammonium bromide
ΔG^0_m	Standard free energy of micelle formation
ΔH^0_m	Standard enthalpy of micelle formation
ILs	Ionic liquids
ILBS	Ionic-liquid-based surfactant
MO	Methyl orange
N_{agg}	Micelle average aggregation number
pC_{20}	Surface adsorption efficiency
ΔS^0_m	Standard entropy of micelle formation
β	Fraction of micelle-bound counter-ion
γ	Surface tension
γ_{cmc}	Surface tension at cmc

Electronic supplementary material The online version of this article (doi:10.1007/s00396-015-3746-x) contains supplementary material, which is available to authorized users.

✉ Naved I. Malek
navedmalek@yahoo.co.in

✉ Omar A. El Seoud
elseoud@iq.usp.br

[1] Applied Chemistry Department, S.V. National Institute of Technology, Surat 395 007, Gujarat, India

[2] Institute of Chemistry, The University of São Paulo, Box 26077, São Paulo, SP 05513-970, Brazil

Γ_{max}	Maximum surface excess concentration
π_{cmc}	Surface pressure at cmc

Introduction

Ionic liquids (ILs) have unique and useful physico-chemical properties, e.g., negligible vapor pressure and high chemical and thermal stability; they are efficient solvents for inorganic and organic substances, and biopolymers [1, 2]. Focusing on imidazole-based ILs, the attachment of at least one long chain, e.g., C_{10} to C_{16}, to the imidazolium ring results in compounds that are surface active and, hence, are termed ionic-liquid-based surfactants, ILBSs [3–25]. Owing to their structural flexibility, ILs were employed in diverse fields, including catalysis [26, 27], nanotechnology [28–30], biomedical applications [31, 32], organic synthesis [2, 26], ion-gel formation [33, 34], drug delivery, extraction, and biotechnological processes [35–40]. The aggregation behavior of ILBSs with different head groups, including amino acid cations, imidazolium, pyridinium, piperidinium, and pyrrolidinium heterocycle, was investigated [1–25, 41]. Tailor-made ILBSs were synthesized by incorporating specific functional groups in their structures, and their aggregation behaviors were compared with "conventional" surfactants [42–45].

In principle, it is possible to alter the balance between hydrophobic/hydrophilic and, where applicable, electrostatic interactions by judicious selection of the head group, the length of the hydrophobic tail, and by incorporating a functional group in the surfactant structure [43–50]. For example, Incorporation of a double bond (db) in the long alkyl chain makes the hydrophobic tail shorter, and less hydrophobic than that of the saturated counterpart. The reason is that db is shorter, and less hydrophobic than the single (C–C) bond [51, 52]. Additionally, packing of the db-carrying chains in the micellar core is hindered because of the rigidity of the unsaturated moiety [53]. Several authors have reported increase in the value of critical micelle concentration (cmc) upon introducing db, including at terminus of the hydrophobic tail, or close to the head group of ionic surfactants [54–61].

We carried out the present study as a part of our interest in assessing the effects of the presence of db on the aggregation of ILBSs; see Fig. ESM-1 (Fig. 1 of Electronic Supplementary Material). Herein, we report on the synthesis and aggregation behavior in aqueous solution at 298.15 K of the series 1-(n-alkyl)-3-vinylimidazolium bromide, C_nVnImBr (n=10, 12, 14, and 16). We studied the adsorption of these surfactants at aqueous solution/air interface and their micellization by surface tension measurements. Conductivity measurements were used to determine the values of their critical micelle concentration (cmc), degree of counter-ion binding (β), and the thermodynamic parameters of micellization (from measurements in the range 298.15 to 313.15 K). Additional information on the formed micelles, e.g., micellar aggregation number (N_{agg}), was obtained from fluorescence quenching of micelle-solubilized pyrene. The effect of the presence of db in the head group on micellar properties was assessed by comparing the aggregation of C_{16}VnImBr with the saturated counterpart (C_{16}EtImBr; Et = ethyl). Where appropriate, we compare the results of the present series with those of other ILBSs, 1-(n-alkyl)-3-methylimidazolium bromides, C_nMeImBr, and "conventional" cationic surfactant N-(n-alkyl)-N,N,N-trimethylammonium bromides, C_nMe_3ABr.

Materials and methods

Materials

1-Vinylimidazole (99 %), 1-ethylimidazole (99 %), 1-bromodecane (98 %), 1-bromododecane, (97 %), 1-bromotetradecane (98 %), and 1-bromohexadecane (97 %) were purchased from Sigma-Aldrich. Pyrene (Merck, 96 %), methyl orange (Acros, 95 %), ethyl acetate (Rankem, 99 %), and diethyl ether (Rankem, 99 %) were used as received. All aqueous solutions were prepared using deionized water.

Synthesis of ILs C_nVnImBr and C_{16}EtImBr

We synthesized the C_nVnImBr surfactants as reported elsewhere [62–65] with several modifications. In brief, we slowly added (3 h), under stirring, a solution of 1-bromoalkane in ethyl acetate (23 mmol in 80 mL) to a solution of 1-vinylimidazole in the same solvent (20 mmol in 60 mL). The reaction temperature was maintained 0 °C throughout the addition. After completion, the reactant mixture was stirred for further 48 h at 50 °C. The progress of the reaction was monitored by TLC (chloroform/methanol, 4:1 by volume). After the completion of the reaction, ethyl acetate was removed and the resulting solid was washed several times with diethyl ether and then dried under reduced pressure at 50 °C until constant weight.

The synthesized ILBSs were characterized by proton nuclear magnetic resonance (^{1}H NMR) spectroscopy (Bruker Avance-II 400 spectrometer, $CDCl_3$), Fourier transform infrared (FTIR) spectroscopy (PerkinElmer Spectrum RX-IFTIR spectrometer; KBr pellet), and elemental analysis (Thermo Electron-Flash EA 1112- CHNS analyzer).

C_{10}VnImBr Light yellow liquid; yield = 82 %. ^{1}H-NMR (δ in ppm): 0.87 (3H, t, N-$(CH_2)_9$-CH_3), 1.20–1.34 (14H, m, N-CH_2-CH_2-$(CH_2)_7$-CH_3), 1.92–1.98 (2H, m, N-CH_2-CH_2-$(CH_2)_7$-CH_3), 4.43 (2H, t, N-CH_2-CH_2-$(CH_2)_7$-CH_3), 5.37–5.40 (1H, dd, CH=CH_2), 6.08–6.12 (1H, dd, CH=CH_2), 7.49–7.55 (1H, dd, CH=CH_2), 7.80 (1H, d, N-CH-CH), 8.18 (1H, d, N-CH-CH), and 10.60 (1H, s, N-CH-N). FTIR, ν_{max}/

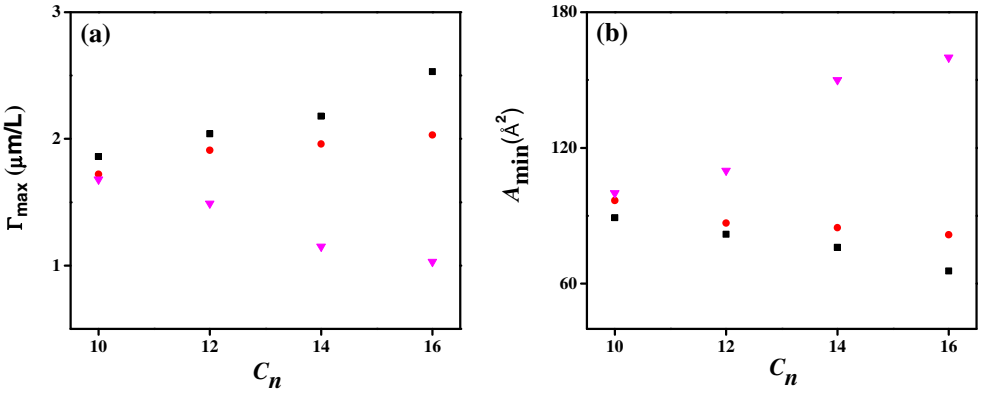

Fig. 1 **a** Γ_{max} and **b** A_{min} of various surfactant series as a function of number of the number of carbon atom in the hydrophobic chain. The symbols employed are as follows: *black square*, $C_nVnImBr$; *red circle*, $C_nMeImBr$ [8, 17]; and *pink inverted triangle*, C_nMe_3ABr [73]

cm^{-1}: ν-CH_2 2928, 2838, ν-CH=CH_2 1650, imidazole ring 1551. Elemental analysis: Analyzed: C 57.08, H 8.55, N 8.75; calculated: C 57.14, H 8.63, N 8.88.

C_{12}VnImBr White solid, m.p. = 47 °C (literature m.p. = 47 °C) [66]; yield = 87 %. ^{1}H-NMR: 0.87 (3H, t, N-$(CH_2)_{11}$-CH_3), 1.24–1.34 (18H, m, N-CH_2-CH_2-$(CH_2)_9$ CH_3), 1.94–1.97 (2H, m, N-CH_2-CH_2-$(CH_2)_9$-CH_3), 4.42 (2H, t, N-CH_2-CH_2-$(CH_2)_9$-CH_3), 5.37–5.50 (1H, dd, CH=CH_2), 6.07–6.11 (1H, dd, CH=CH_2), 7.49–7.55 (1H, dd, CH=CH_2), 7.79 (1H, d, N-CH-CH), 8.17 (1H, d, N-CH-CH), and 10.56 (1H, s, N-CH-N). FTIR, ν_{max}/cm^{-1}: ν-CH_2 2917, 2850, ν-CH=CH_2 1650, imidazole ring 1552. Elemental analysis: Analyzed: C 59.33, H 9.03, N 8.10; calculated: C 59.47, H 9.10, N 8.16.

C_{14}VnImBr White solid, m.p. = 62 °C; yield: 84 %. ^{1}H-NMR: 0.87 (3H, t, N-$(CH_2)_{13}$-CH_3), 1.24-1.34 (22H, m, N-CH_2-CH_2-$(CH_2)_{11}$-CH_3), 1.92–1.99 (2H, m, N-CH_2-CH_2-$(CH_2)_{11}$-CH_3), 4.20 (2H, t, N-CH_2-CH_2-$(CH_2)_{11}$-CH_3), 5.37–5.40 (1H, dd, CH=CH_2), 6.05–6.10 (1H, dd, CH=CH_2), 7.49–7.52 (1H, dd, CH=CH_2), 7.75 (1H, d, N-CH-CH), 8.13 (1H, d, N-CH-CH), and 10.62 (1H, s, N-CH-N). FTIR, ν_{max}/cm^{-1}: ν-CH_2 2917, 2849, ν-CH=CH_2 1650, imidazole ring 1551. Elemental analysis: Analyzed: C 61.23, H 9.42, N 7.37; calculated: C 61.44, H 9.50, N 7.54.

C_{16}VnImBr White solid, m.p. = 69 °C; yield: 81 %. (literature mp = 69 °C [67]) ^{1}H-NMR: 0.87 (3H, t, N-$(CH_2)_{15}$-CH_3), 1.24–1.34 (26H, m, N-CH_2-CH_2-$(CH_2)_{13}$ CH_3), 1.91–1.99 (2H, m, N-CH_2-CH_2-$(CH_2)_{13}$-CH_3), 4.41 (2H, t, N-CH_2-CH_2-$(CH_2)_{13}$-CH_3), 5.37–5.40 (1H, dd, CH=CH_2), 6.02–6.07 (1H, dd, CH=CH_2), 7.35–7.54 (1H, dd, CH=CH_2), 7.68 (1H, d, N-CH-CH), 8.05 (1H, d, N-CH-CH), and 10.69 (1H, s, N-CH-N). FTIR, ν_{max}/cm^{-1}: ν-CH_2 2917, 2849, ν-CH=CH_2 1650, imidazole ring 1551. Elemental analysis: Analyzed: C 63.06, H 9.71, N 6.93; calculated: 63.14, H 9.84, N 7.01.

1-(n-Hexadecyl)-3-ethylimidazolium bromide C_{16}EtImBr was synthesized according to the procedure reported earlier [63]. Briefly, a mixture of 1-ethylimidazole (10.4 mmol) and 1-bromohexadecane (10.4 mmol) in 120 ml of 2-propanol was maintained under reflux with constant stirring for 24 h. The solvent was removed, and the solid product was dissolved in water and extracted five times by ethyl acetate. Finally, water was evaporated under reduced pressure at 80 °C, and the product was dried in a vacuum oven for 48 h.

C_{16}EtImBr White solid, m.p. = 56 °C; yield: 81 %. (literature mp = 55.7 °C [63]) (white solid) ^{1}H-NMR: 0.85 (3H, t, N-$(CH_2)_{15}$-CH_3), 1.22–1.29 (26H, m, N-CH_2-CH_2-$(CH_2)_{13}$ CH_3), 1.56 (3H, t, CH_2-CH_3), 1.88 (2H, m,CH_3-CH_2), 1.88–1.92 (2H, m, N-CH_2-CH_2-$(CH_2)_{13}$-CH_3), 4.24 (2H, t, N-CH_2-CH_2-$(CH_2)_{13}$-CH_3), 5.22–5.30 (1H, dd, CH=CH_2), 5.98–6.02 (1H, dd, CH=CH_2), 7.35–7.54 (1H, dd, CH=CH_2), 7.60 (1H, d, N-CH-CH), 7.95 (1H, d, N-CH-CH), and 10.35 (1H, s, N-CH-N). FTIR, ν_{max}/cm^{-1}: ν-CH_2 2917, 2849, ν-CH 1475, imidazole ring 1551. Elemental analysis Analyzed: C, 60.40; H, 10.60; N, 6.68. Calculated: C, 60.13; H, 10.33; N, 6.68.

Notes Except for conductance, we carried out all measurements at 298.15±0.1 K. In all cases, ILBSs were dried under reduced pressure until constant weight; deionized water was employed throughout.

Measurements

Surface tension measurements

Surface tension measurements were performed using du Noüy ring method and Krüss K9 tensiometer. The concentrations of ILBSs were increased by successive addition of their concentrated solutions. The measured surface tension values (γ±0.1 mN m^{-1}) were corrected according to the procedure of Harkins and Jordan [68], built-in in the instrument software.

Conductivity measurements

Electrical conductivities (κ) were measured at four different temperatures from 298.15 to 313.15 K, in 5-K intervals, by EUTECH PC 6000 digital conductivity meter, having a sensitivity of 0.1 μS cm^{-1} and an accuracy of 0.5 %. The conductivity probe (EC- CONSEN 21B) has a built-in PT-100 temperature sensor; it was calibrated with aqueous KCl solutions (0.01–1.0 mol kg^{-1}). Five measurements were made for each surfactant concentration; the uncertainty of the measurements was <0.3 %.

UV–vis measurements

We used a Varian Cary 50 spectrophotometer, equipped with a thermostated cell compartment. The absorption spectra of solutions containing MO (fixed at 20 μM) plus variable [ILBS] were registered using a 1-cm path length quartz cuvette.

Steady state fluorescence measurements

These were performed using a Jasco FP-6300 spectrofluorimeter, using a 1-cm path length quartz cuvette. Pyrene was used as the polarity probe with fixed concentration of 1 μM in all experiments to avoid perturbing the micelle. The emission spectra of pyrene were recorded in the wavelength range 350–500 nm at an excitation wavelength of 334 nm using the excitation and emission slit widths of 2.5 nm. The first (I_1) and third (I_3) vibronic peaks of pyrene appeared at 373 and 384 nm, respectively. The fluorescence intensities were corrected for the instrumental response. The value of cmc was determined from the dependence of (I_1/I_3) on log [ILBS]; see part Fig. 3b. For the aggregation number, steady state fluorescence quenching measurements were performed using pyrene as probe and cetylpyridinium chloride (CPC) as quencher, by adding a stock solution of ILBS-solubilized pyrene (2.0×10^{-6} M probe) to a stock solution of quencher in water. Prior to the measurements, the mixed solutions were stirred and equilibrated for 2 and 5 min, respectively.

Results and discussion

Notes:

1. The (standard) equations employed to calculate surfactant adsorption and micellization are listed in ESM.
2. The structural variable in the series studied is the chain length of the alkyl group (C_n). Additionally, the ILBS head group carries a db. For ease of reading, we present our data by discussing first the effect of C_n (C_{10}–C_{16}) on the calculated property and compare the present series, where appropriate, with other ILBSs, and conventional surfactants with the same counterion and C_n. In order to show the effect of the db, we compare the data for C_{16}VnImBr with the corresponding ones for C_{16}EtImBr. We selected this C_n because the corresponding cmc's are low, i.e., the solutions can be considered ideal. Consequently, we can attribute any difference between the properties of C_{16}VnImBr and C_{16}EtImBr to the effect of the vinyl group, as compared with the ethyl moiety.
3. We present our data in the order of sequence of events when the ILBS is dissolved in water, i.e., adsorption at solution/air interface and then aggregation as micelles.

Adsorption at solution/air interface

Surface tension measurements provide information about surfactant adsorption at solution/air interface, including surface tension at cmc (γ_{cmc}), adsorption efficiency (pC_{20}), the effectiveness of surface tension reduction (π_{cmc}), the maximum surface excess concentration (Γ_{max}), and the minimum area occupied per ILBS molecule (A_{min}) at solution/air interface [17, 69–72]; these data are reported in Table 1.

As shown in Table 1, the values of γ_{cmc}, a measure of surface activity, decrease as a function of increasing (C_n) the chain length of C_nVnIMBr; γ_{cmc} for C_{16}VnImBr is slightly larger than for C_{16}EtImBr, showing that the db is less hydrophobic than the ethyl group. The values of pC_{20} and π_{cmc} of C_nVnImBr increase with increasing alkyl chain length, similar to the C_nMeImBr series [8, 17]. Such dependence indicates that the adsorption efficiency of ILBSs at solution/air interface increases with increasing C_n, due to an increase in the hydrophobic interactions between ILBS monomers.

Table 1 Dependence of surfactant adsorption parameters at 298.15 K on C_n of ILBSs

ILBS	γ_{cmc} (mN/m)	π_{cmc} π_{cmc} (mN/m)	pC_{20}	$\Gamma_{max}10^6$ (mol/m^2)	A_{min} (Å^2)	ΔG^0_{ads}
C_{10}VnImBr	34.5	37.3	2.44	1.86	89.3	−50.60
C_{12}VnImBr	34.1	38.4	2.80	2.03	81.8	−56.31
C_{14}VnImBr	33.8	38.6	3.40	2.18	76.2	−61.30
C_{16}VnImBr	33.5	39.1	4.00	2.53	65.7	−65.47
C_{16}EtImBr	32.2	40.3	4.22	2.58	64.2	−66.32

The uncertainties in the calculated parameters are as follows: γ_{cmc}= ±0.1 mN/m; π_{cmc}=±0.1 mN/m; Γ_{max}=$\pm0.2\times10^{-6}$ mol/m^2 ; A_{min}=0.5 Å^2

ILBS ionic-liquid-based surfactant

The values of Γ_{max} and A_{min} listed in Table 1 show that the former increases and the latter decreases as a function of increasing (n), similar to $C_nMeImBr$, and conventional cationic surfactants [8, 17, 45, 69, 73]. These results indicate the enhanced hydrophobic interactions and tight packing of the $C_nVnImBr$ monomers. In Fig. 1, we compare the results of three surfactant series, namely, $C_nVnImBr$, $C_nMeImBr$, and C_nMe_3ABr. As shown, Γ_{max} were found to be largest and A_{min} smallest [8, 17, 73] for $C_nVnImBr$. This indicates that more $C_nVnImBr$ molecules adsorb at solution/air interface, which is the result of higher hydrophobic interactions in the vinyl series. On comparing the effect of unsaturation in the head group, $C_{16}EtImBr$ has higher Γ_{max} than the $C_{16}VnImBr$, due to larger hydrophobic character of the former surfactant.

The standard free energy of adsorption (ΔG^0_{ads}), which is the free energy of transfer of 1 mol of surfactant molecules from bulk solution to the surface [69], is negative. The larger values of $|\Delta G^0_{ads}|$ than those of $|\Delta G^0_m|$ (see Table 3) indicate more spontaneous adsorption at the solution/air interface than micellization in the bulk. The difference between $|\Delta Gads^0|$ of $C_{16}VnImBr$ and $C_{16}EtImBr$ can be attributed to the difference between the hydrophobic character of the vinyl and ethyl groups.

Micelle formation

Dependence of the cmc on C_n at 298.15 K

Values of cmc were determined by surface tension and conductivity measurements, and from the spectra of dissolved probes, as follows:

- Plots of surface tension (γ) versus log [ILBS] decreased as a function of increasing the surfactant concentration until the cmc and stayed practically constant at larger log [ILBS]. Values of the cmc were taken where γ became essentially constant, as shown in of Fig. 2a.
- Plots of solution conductivity (κ) versus log [ILBS] showed two straight lines with different slopes, intersecting at the cmc, as shown in Fig. 2b.
- In the experiments with probes, we plotted the dependence of a spectral parameter of the probe on log [ILBS]. As shown in Fig. 3a, the dependence of the ultraviolet–visible (UV–vis) absorbance of MO on log [ILBS] is sigmoidal. We calculated the cmc from the inflection point in the derivative curve (∂(absorbance)/∂ log [ILBS]) versus log [ILBS], as shown in Fig. ESM-3. As shown in Fig. 3b, the dependence of the intensity ratio of the first and third vibronic peaks of pyrene (I_1/I_3) on log [ILBS] showed two lines, intersecting at the cmc. Table 2 shows the cmc values, calculated from the data of these independent techniques.

The agreement between the results of distinct techniques is satisfactory, taking into account that these are sensitive to different aspects of the micellization process and the fact that cmc calculated from probe solubility maybe slightly different due to probe–monomer association before the cmc (vide infra the discussion on solubilization of MO). The reasons for the observed dependence of cmc on the technique employed have been discussed elsewhere [74]. For example, Mukerjee and Mysels have compiled 54 cmc's for $C_{16}Me_3ABr$ (measurements at 25 °C), differing, for the same technique, by 22% [75]!

Another way of assessing the effect of the vinyl moiety in the surfactant head group is Fig. 4, which depicts the cmc values of the $C_nVnImBr$ (present work), $C_nMeImBr$ [8, 17], and C_nMe_3ABr [69, 70, 76, 77] series. As the insert shows, the order of cmc is $C_nMe_3ABr > C_nVnImBr$ and, as shown above, $C_{16}EtImBr > C_{16}VnImBr$. Except for $C_{10}VnImBr$, the cmc values of the $C_nVnImBr$ and $C_nMeImBr$ series are similar, i.e., the effect of the vinyl moiety on cmc is akin to introducing one carbon atom in the head group (CH_3), in agreement with the less hydrophobic character of the vinyl group, relative to the ethyl group.

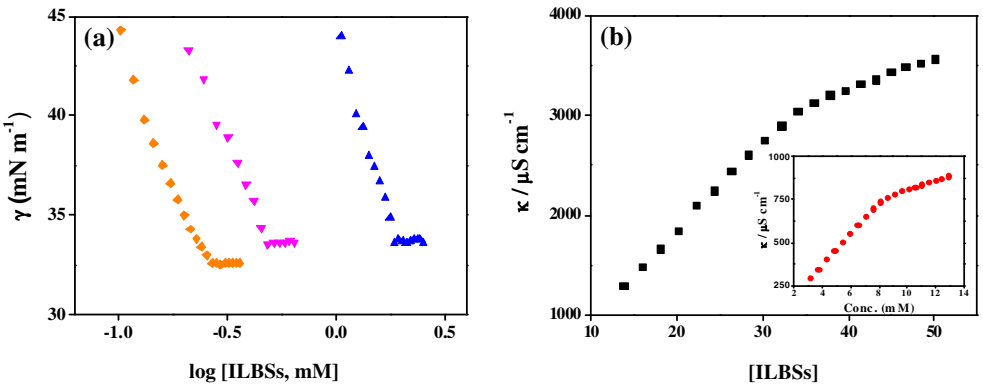

Fig. 2 Representative plots of the dependence of surface tension (γ; **a**) and specific conductance (κ; **b**) on surfactant concentration in millimolars, at 298.15 K. The symbols are as follows: *blue upright triangle*, $C_{14}VnImBr$; *pink inverted triangle*, $C_{16}VImBr$; *orange diamond*, $C_{16}EtImBr$; *black square*, $C_{10}VnImBr$; and *red circle*, $C_{12}VnImBr$

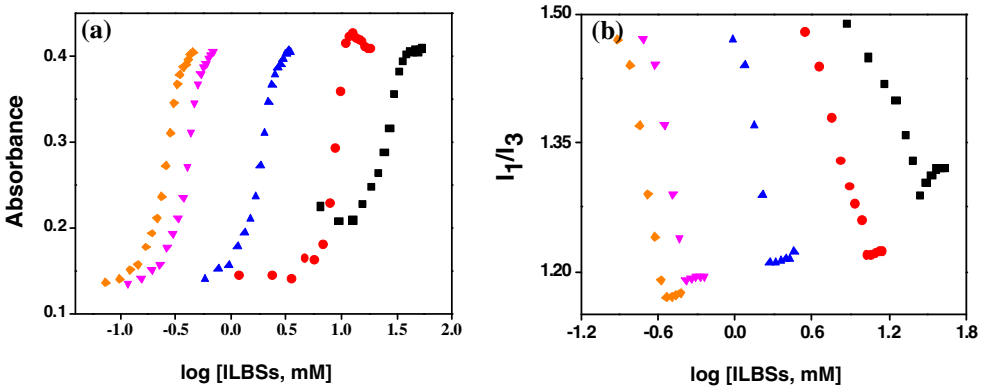

Fig. 3 Dependence of UV–vis absorption of solubilized MO (**a**) and the ratio of the first and third vibronic peaks of solubilized pyrene (I_1/I_3; **b**) on surfactant concentration in millimolars, at 298.15 K. The symbols are as follows: *black square*, C_{10}VnImBr; *red circle*, C_{12}VnImBr; *blue upright triangle*, C_{14}VnImBr; *pink inverted triangle*, C_{16}VnImBr; and *orange diamond*, C_{16}EtImBr

According to the Stauff-Klevens rule [78–80], the relationship between cmc and the number of carbon atoms in the alkyl chain is given by

$$\log cmc = A - B\ C_n \quad (1)$$

where A and B are constants for a particular homologous series. The constant A varies with the nature and number of head groups per surfactant monomer, whereas B measures the effect of each additional methylene group on cmc. It represents the free energy of the transfer of a methylene group from bulk to micellar pseudo-phase. We applied Eq. 1 for the data obtained from conductance and obtained excellent straight lines with slopes of −0.3± 0.05 and correlations coefficients of ~0.999. These results are similar to those obtained for C_nMeImBr and C_nMe$_3$ABr [81]. For all these series, the value of B is close to log 2, meaning that addition of a methylene group to the hydrocarbon chain decreases the cmc of by approximately a factor of 2 [82].

Dependence of cmc on the temperature: calculation of the thermodynamic parameters of micellization

From conductance data at different temperatures (298.15, 303.15, 308.15, and 313.15 K), we calculated the cmc, β, and thermodynamic parameters of micelle formation; see Table 3. For each studied ILBS, the cmc increases as a function of increasing T. The two contributing factors for such behavior are (i) decreasing hydration of the surfactant head group, favoring micellization, and (ii) breaking of the water structure around the hydrophobic part, which increases the solubilization of monomers and disfavors the micellization. In the present study, the second factor is dominant.

At a fixed T, the value of β increases with increasing the alkyl chain length for C_nVnImBr, due to the corresponding increase in hydrophobic interactions. A similar observation was reported for the C_nMeImBr and for C_nMe$_3$ABr [4, 11, 69–72, 76, 77]. For the same alkyl chain length, β follows the order C_nVnImBr < C_nMeImBr < C_nMe$_3$ABr [69, 70, 76, 77]. The decreasing β values with increasing T indicates that the charge density on the micellar surface is decreasing, due to increased thermal motion of the surfactant ions [36]. Recently, Kamboj et al. observed a decrease in β with increasing alkyl chain length for the morpholinium-based amide-functionalized ILBSs in aqueous media [44]. The same result was observed for conventional

Table 2 Values of cmc determined by different experimental techniques for ILBSs, at 298.15 K

ILBS	cmc (mM)			
	ST	Cond.	UV–vis	Fluor
[C_{10}VnImBr]	27.20	33.22	26.86	24.13
[C_{12}VnImBr]	7.00	8.17	8.75	11.33
[C_{14}VnImBr]	1.85	2.06	1.85	1.86
[C_{16}VnImBr]	0.48	0.49	0.40	0.41
[C_{16}EtImBr]	0.26	0.27	0.26	0.29

ILBS ionic-liquid-based surfactant, *ST* surface tension, *Cond* conductance, *UV–vis* UV–vis absorption of MO, *Fluor* fluorescence of pyrene

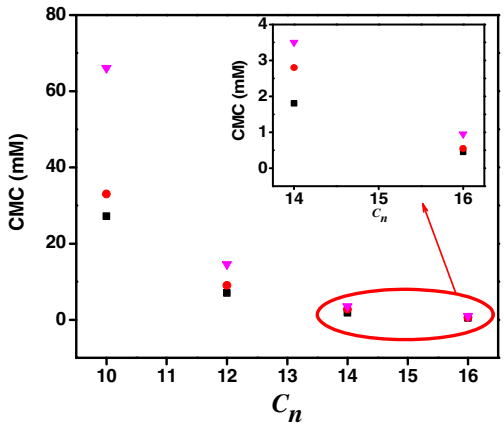

Fig. 4 Dependence of the cmc values on the structure of the head group. The symbols are as follows: *black square*, C_nVnImBr; *red circle*, C_nMeImBr; and *pink inverted triangle*, C_nMe$_3$ABr

Table 3 Dependence of the critical micelle concentration (cmc), degree of counter-ion association (β), free energy (ΔG_m^0), enthalpy (ΔH_m^0), and entropy (ΔS_m^0) of micelle formation on the structure of the surfactants studied and the temperature (T)

ILBS	Temp. (K)	cmc (mM)	β	ΔG_m^0 (kJ mol^{-1})	ΔH_m^0 (kJ mol^{-1})	ΔS_m^0 (J mol^{-1}k^{-1})	Λ_0 (S cm^2 mol^{-1})
C_{10}VnImBr	298.15	33.22	0.65	−30.34	−4.87	85.41	29.9
	303.15	33.79	0.63	−30.41	−4.98	83.88	-
	308.15	34.39	0.61	−30.46	−5.08	82.34	-
	313.15	35.28	0.59	−30.47	−5.18	80.72	-
C_{12}VnImBr	298.15	8.17	0.70	−37.33	−8.83	95.60	25.5
	303.15	8.27	0.68	−37.38	−9.00	93.61	-
	308.15	8.56	0.67	−37.54	−9.22	91.88	-
	313.15	8.93	0.66	−37.74	−9.47	90.27	-
C_{14}VnImBr	298.15	2.06	0.72	−43.59	−10.19	112.02	21.1
	303.15	2.13	0.71	−43.81	−10.45	110.05	-
	308.15	2.20	0.69	−43.89	−10.67	107.79	-
	313.15	2.34	0.64	−43.00	−10.69	103.17	-
C_{16}VnImBr	298.15	0.49	0.73	−50.02	−11.53	129.07	18.3
	303.15	0.51	0.65	−48.40	−11.38	122.10	-
	308.15	0.53	0.62	−48.22	−11.57	118.94	-
	313.15	0.56	0.57	−47.11	−11.54	113.60	-
C_{16}EtImBr	298.15	0.27	0.67	−50.70	-	-	16.3

ILBS ionic-liquid-based surfactant

cationic and anionic surfactants and may be traced to increased mobility and hydration of the head-ions [44, 83–85].

The thermodynamics parameters of micellization (ΔG_m^0, ΔH_m^0, and (ΔS_m^0) were calculated using the pseudo phase model, and the values are listed in Table 3. The increase of $|\Delta G_m^0|$ with the chain length indicates the dominating hydrophobic interactions [35], and the order of $|\Delta G_m^0|$ is C_{16}MeImBr ≈ C_{16}VnImBr > C_{14}VnImBr > C_{12}VnImBr > C_{10}VnImBr. Furthermore, ΔH_m^0 values are negative at each T (Table 3), i.e., micelle formation is an exothermic process and slightly increases with temperature, indicating that temperature has less impact on the hydrophobic part of ILBSs in aqueous solution [18]. Such phenomena occur in the system where the principle force of micellization is the London dispersion interactions [86]. The notable positive values of ΔS_m^0 indicate that micelle formation is entropy-driven rather than enthalpy-driven [5, 36]. After micellization, the hydrophobic part of the monomer including vinyl group interacts with each other and excludes water from the micellar core, which increases the entropy of the system [42].

From the limiting equivalent conductivity (Λ_0) for C_nVnImBr (Fig. ESM-2), and Λ_0 for the Br^- ion, 78.1 S cm^2 mol^{-1} [85], we calculated the values of Λ_0 (C_nVnIm$^+$) shown in Table 3. It decreases with increasing C_n, due to the concomitant reduction in cation mobility of ILBSs [87]. The values of Λ_0 for C_nVnIm$^+$ are lower than the corresponding values for C_nMeIm$^+$ [87]. On comparing the values for Λ_0 (C_{16}VnIm$^+$) with Λ_0 (C_{16}Eim$^+$), it was observed that incorporating the unsaturation in the head group increases the Λ_0.

Table 4 Dependence of the aggregation number (N_{agg}) and intensity ratio of the first and third vibronic peaks of pyrene (I_1/I_3) on the chain length of ILBSs, and calculated dielectric constants (ε) for the average solubilization sites of micelle-solubilized pyrene, at 298.15 K

Property	ILBS				
	C_{10}VnImBr	C_{12}VnImBr	C_{14}VnImBr	C_{16}VnImBr	C_{16}EtImBr
N_{agg}	32	42	47	54	60
I_1/I_3	1.28	1.22	1.21	1.19	1.17
ε	22.3	17.5	16.7	15.1	13.5

ILBS ionic-liquid-based surfactant

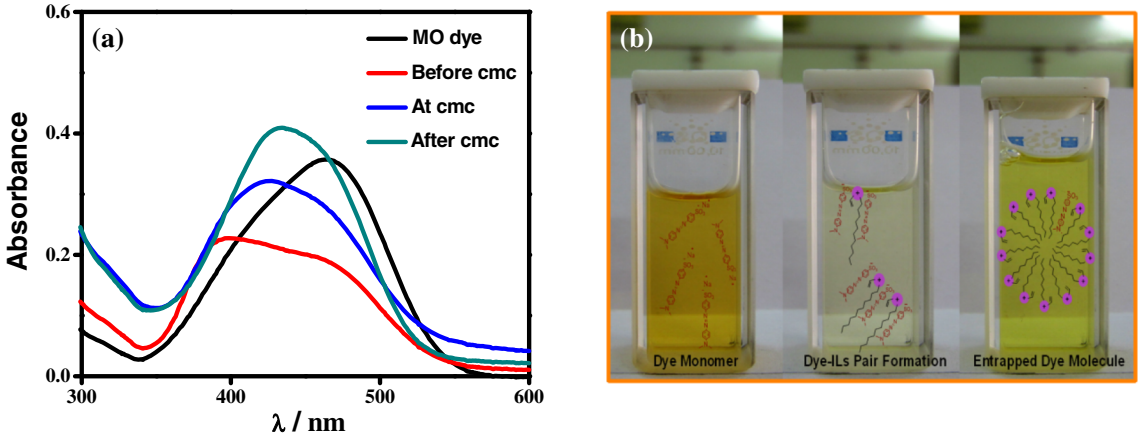

Fig. 5 Dependence of UV–vis spectra and solution colors of MO on the concentration of C_nVnImBr, in aqueous solution, at 298.15 K

Micelle aggregation numbers and properties of the interfacial region

The aggregation numbers (N_{agg}) increase with increasing chain length from C_{10}VnImBr to C_{16}VnImBr; they are lower than the corresponding ones for C_nMeImBr, 42, 44, 59, and 66, for C_n=10, 12, 14, and 16, respectively [4, 8]. The same trend is observed for C_nMe_3ABr, 40, 55, 70, and 89, for C_n=10, 12, 14, and 16, respectively [88]. Furthermore, N_{agg} values are in the order C_{16}EtImBr > C_{16}VnImBr (Table 4). The lower N_{agg} of C_nVnImBr is attributed to the more rigid nature of the vinyl group which does not permit efficient packing in the micelle.

For pyrene solubilized in micellar C_nVnImBr, with increasing the alkyl chain length from C_{10} to C_{16}, I_1/I_3 values decrease from 1.28 to 1.19 (Table 4), similar to the C_nMeImBr and C_nMe_3ABr micelles [4]. Furthermore, the order of I_1/I_3 is C_nVnImBr < C_nMeImBr [4], which shows that pyrene resides in less polar environment in the vinyl group containing ILBSs than in the C_nMeImBr series. The I_1/I_3 value for C_{16}VnImBr is higher than that for C_{16}EtImBr, which confirms the less hydrophobic character of the unsaturated bearing head group.

We calculated the apparent dielectric constant (ε) of the (average) micellar solubilization site of pyrene from the following relation [89]:

$$I_1/I_3 = 1.000461 + 0.01253\varepsilon \quad (2)$$

As reported in Table 4, with increasing the alkyl chain length in C_nVnImBr, solubilized pyrene experiences more nonpolar environment. The unsaturation in the C_{16}VnImBr leads to higher value for ε, as compared with that in C_{16}EtImBr.

Solubilization of methyl orange

Analysis of the UV–vis absorbance of MO in the presence of ILBSs (both in monomer and micellar regions) gave interesting results because the dye and ILBS carry opposite charges [90–95]. In pure solvents, the sensitivity of the value λ_{max} of MO to medium polarity is shown by the following values of λ_{max}: 462, 442, 417, 412, and 396 nm, for water, ethylene glycol, ethanol, acetone, and heptane, respectively [94]. We used this sensitivity to assess the solubilization of MO in the surfactant solution. [90–95]. Our results are depicted in Fig. 5 and Table 5.

As shown by these results, λ_{max} of the dye shows a blue shift (relative to water) as a function of increasing [C_{16}VnImBr], most certainly because of dye–surfactant association. This anion–cation interaction decreases dye

Table 5 Dependence of λ_{max} of MO on [C_nVnImBr] and [C_{16}EtImBr] ILBSs in aqueous solutions at 298.15 K

	λ_{max} (nm)				
	[C_{10}VnImBr]	[C_{12}VnImBr]	[C_{14}VnImBr]	[C_{16}VnImBr]	[C_{16}EtImBr]
Dye in water	463	463	463	463	463
Before cmc	396	379	372	370	368
At cmc	425	422	419	412	408
After cmc	433	429	429	429	429

cmc critical micelle concentration

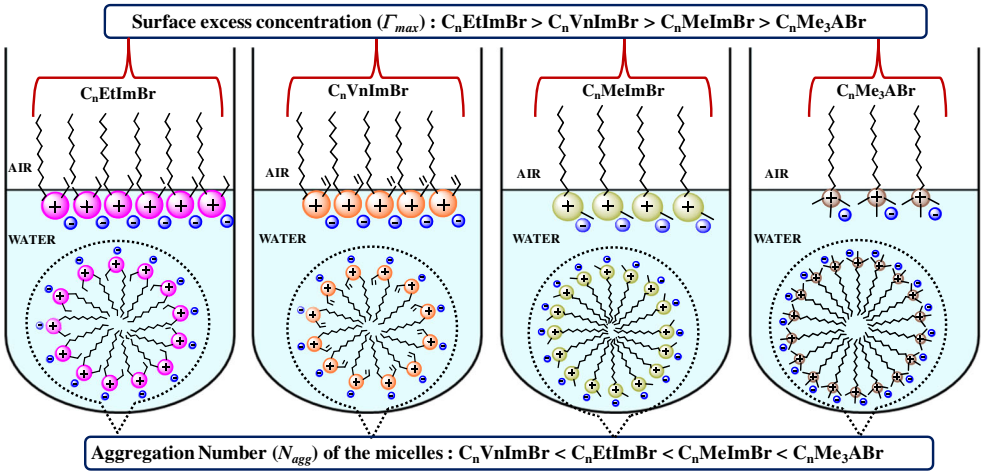

Fig. 6 A graphic summary of our results for four surfactant series

hydration, i.e., results in a decrease in the polarity of the dye solvation shell [94]. Additionally, dye–surfactant interactions result in decreasing the electrostatic repulsion between dye molecules. This possibly leads to formation of dye dimeric or trimeric species [94, 96] at concentration below the cmc, and visible change in the dye color, see Fig. 5. When more surfactant is added, MO dimers and trimers disappear [96, 97]; the dye shows red shift, and a change in absorbance (manifested by a color change).

We envisage that the MO molecule is aligned parallel with the alkyl chain of the ILBS, with its sulfonate group anchored to the cationic head group of the ILBS [91]. The decrease in λ_{max} with increasing C_n is consistent with the more hydrophobic environment for the probe molecule as a consequence of more extensive "enclosure" by a longer alkyl tail. After the formation of the probe–ILBS complex, once the dye molecules are entrapped in the micelle, their absorbance becomes insensitive to increasing [ILBS], i.e., λ_{max} stays constant (except for C_{10}VnImBr). The difference between the vinyl and ethyl groups is manifested in the values of λ_{max}, before or at the cmc.

Conclusions

Structural modification of ILBSs by incorporating unsaturation in the head group leads to an increase in cmc, relative to C_{16}EtImBr, due to the less hydrophobic character of the vinyl group, relative to the ethyl moiety. We obtained information on the adsorption, and micellization of C_nVnImBr in aqueous solutions from surface tension, conductivity, UV–vis, and fluorescence of solubilized dyes. From the results obtained, we calculated surface adsorption parameters (pC_{20}, π_{cmc}, and Γ_{max}). These are higher as compared to those for C_nMeImBr, which indicates that C_nVnImBr is more surface active. Thermodynamic parameters of micellization were evaluated using the temperature dependence of cmc and counter-ion binding β. The thermodynamic parameters indicated that micellization is entropy-driven. Methyl orange (MO) was used as a probe to investigate the dye aggregation behavior, and formation of MO–ILBS complexes prior to and after the cmc. Steady state fluorescence and pyrene fluorescence quenching were used to calculate the cmc and N_{agg} of the ILBSs, respectively. Values of cmc obtained from all four techniques are in good agreement with each other. cmc's of the studied ILBSs are lower as compared to those for C_nMeImBr and C_nMe_3ABr. We show a graphic summary of these results in Fig. 6.

Acknowledgments We thank FAPESP (São Paulo State Research Foundation) for financial support of this work and a PD fellowship to N. I. Malek; CNPq (National Council for Scientific and Technological Research) for a research productivity fellowship to O. A. El Seoud, Maulana Azad National Fellowship (MANF-2012-13-MUS-GUJ-10818) for a research fellowship to Z. Vaid, and TEQIP fellowship to U. More.

References

1. Roger RD, Seddon KR (2003) Ionic Liquids as Green Solvents: Progress and Prospects, American Chemical Society, Washington, D.C.
2. Wasserscheid P, Welton T (2003) Ionic liquids in syntheses. VCH-Wiley, New York
3. Jungnickel C, Luczak J, Ranke J, Fernandez JF, Muller A, Thoming J (2008) Micelle formation of imidazolium ionic liquids in aqueous solution. Colloids Surf A Physicochem Eng Asp 316:278–284. doi: 10.1016/j.colsurfa. 2007.09.020
4. Vanyur R, Biczok L, Miskolczy Z (2007) Micelle formation of 1-alkyl-3-methylimidazolium bromide ionic liquids in aqueous solution. Colliods Surf A Physicochem Eng Asp 299:256–261
5. Luczak J, Jungnickel C, Joskowska M, Thoming J, Hupka J (2009) Thermodynamics of micellization of imidazolium ionic liquids in aqueous solutions. J Colloid Interface Sci 336:111–116
6. Zhang H, Li K, Liang H, Wang J (2008) Spectroscopic studies of the aggregation of imidazolium-based ionic liquids. Colloids Surf A Physicochem Eng Asp 329:75–81

7. Cornellas A, Perez L, Comelles F, Ribosa I, Manresa A, Garcia MT (2010) Self-aggregation and antimicrobial activity of imidazolium and pyridinium based ionic liquids in aqueous solution. J Colloid Interface Sci 355:164–171
8. Dong B, Zhao X, Zheng LQ, Zhang J, Li N, Inoue T (2008) Aggregation behavior of long-chain imidazolium ionic liquids in aqueous solution: micellization and characterization of micelle microenvironment. Colloids Surf A Physicochem Eng Asp 317:666–672
9. Geng F, Liu J, Zheng L, Yu L, Li Z, Li G, Tung C (2010) Micelle formation of long-chain imidazolium ionic liquids in aqueous solution measured by isothermal titration microcalorimetry. J Chem Eng Data 55:147–151
10. El Seoud OA, Pires PAR, Abdel-Moghny T, Bastos EL (2007) Synthesis and micellar properties of surface-active ionic liquids: 1-alkyl-3-methylimidazolium chlorides. J Colloid Interface Sci 313:296–304
11. Inoue T, Ebina H, Dong B, Zheng L (2007) Electrical conductivity study on micelle formation of long-chain imidazolium ionic liquids in aqueous solution. J Colloid Interface Sci 314:236–241
12. Sastry NV, Vaghela NM, Aswal VK (2012) Effect of alkyl chain length and head group on surface active and aggregation behavior of ionic liquids in water. Fluid Phase Equilib 327:22–29
13. Wang H, Wang J, Zhang S, Xuan X (2008) Structural effects of anions and cations on the aggregation behavior of ionic liquids in aqueous solutions. J Phys Chem B 112:16682–16689
14. Blesic M, Lopes A, Melo E, Petrovski Z, Plechkova NV, Canongia Lopes JN, Seddon KR, Rebelo LPN (2008) On the self-aggregation and fluorescence quenching aptitude of surfactant ionic liquids. J Phys Chem B 112:8645–8650
15. Singh T, Kumar A (2007) Aggregation Behavior of Ionic Liquids in Aqueous Solutions: Effect of Alkyl Chain Length, Cations and Anions. J Phys Chem B 111:7843–7851
16. Vaghela NM, Sastry NV, Aswal VK (2011) Surface active and aggregation behavior of methylimidazolium-based ionic liquids of type [$C_n$mim] [X], n=4, 6, 8 and [X]=Cl^-, Br^-, and I^- in water. Colloid Polym Sci 289:309–322
17. Dong B, Li N, Zheng L, Yu L, Inoue T (2007) Surface adsorption and micelle formation of surface active ionic liquids in aqueous solution. Langmuir 23:4178–4182
18. Ao M, Kim D (2013) Aggregation behavior of aqueous solutions of 1-Dodecyl-3-methylimidazolium salts with different halide anions. J Chem Eng Data 58:1529–1534
19. Anouti M, Jones J, Boisset A, Jacquemin J, Caravanier MC, Lemordant D (2009) Aggregation behavior in water of new imidazolium and pyrrolidinium alkycarboxylates protic ionic liquids. J Colloid Interface Sci 340:104–111
20. Rather MA, Rather GM, Pandit SA, Bhat SA, Bhat MA (2015) Determination of cmc of imidazolium based surface active ionic liquids through probe-less UV–vis spectrophotometry. Talanta 131:55–58
21. Cheng N, Ma X, Sheng X, Wang T, Wang R, Jiao J, Yu L (2014) Aggregation behavior of anionic surface active ionic liquids with double hydrocarbon chains in aqueous solution: Experimental and theoretical investigations. Colloids Surf A Physicochem Eng Asp 453:53–61
22. Modaressi A, Sifaoui H, Mielcarz M, Domanska U, Rogalski M (2007) Influence of the molecular structure on the aggregation of imidazolium ionic liquids in aqueous solutions. Colloids Surf A Physicochem Eng Asp 302:181–185
23. Wang X, Liu J, Yu L, Jiao J, Wang R, Sun L (2013) Surface adsorption and micelle formation of imidazolium-based zwitterionic surface active ionic liquids in aqueous solutions. J Colloid Interface Sci 391:103–110
24. Singh T, Rao KS, Kumar A (2012) Effect of ethylene glycol and its derivatives on the aggregation behavior of an ionic liquid 1-butyl-3-methylimidazolium octyl sulfate in aqueous medium. J Phys Chem B 116:1612–1622
25. Blesic M, Marques MH, Plechkova NV, Seddon KR, Rebelo LPN, Lopes A (2007) Self-aggregation of ionic liquids: micelle formation in aqueous solution. Green Chem 9:481–490
26. Choi YS, Shim YN, Lee J, Yoon JH, Hong CS, Cheong M, Kim HS, Jang HG, Lee JS (2011) Ionic liquids as benign catalysts for the carbonylation of amines to formamides. Appl Catal A Gen 404:87–92
27. Wang A, Zheng X, Zhao Z, Li C, Cui Y, Zheng X, Yin J, Yang G (2014) Bronsted acid ionic liquids catalyzed Friedel–Crafts Alkylations of electron-rich arenes with aldehydes. Appl Catal A Gen 482:198–204
28. Bussamara R, Melo WWM, Scholten JD, Migowski P, Marin G, Zapata MJM, Machado G, Teixeira SR, Novak MA, Dupont J (2013) Controlled synthesis of Mn_3O_4 nanoparticles in ionic liquids. Dalton Trans 42:14473–14479
29. Kim KS, Demberelnyamba D, Lee H (2004) Size-selective synthesis of gold and platinum nanoparticles using novel thiol-functionalized ionic liquids. Langmuir 20:556–560
30. Schutte K, Meyer H, Gemel C, Barthel J, Fischer RA, Janiak C (2014) Synthesis of Cu, Zn and Cu/Zn brass alloy nanoparticles from metal amidinate precursors in ionic liquids or propylene carbonate with relevance to methanol synthesis. Nanoscale 6:3116–3126
31. Yang X, Zhang S, Yu W, Liu Z, Lei L, Li N, Zhang H, Yu Y (2014) Ionic liquid-anionic surfactant based aqueous two-phase extraction for determination of antibiotics in honey by high-performance liquid chromatography. Talanta 124:1–6
32. Khan AB, Ali M, Malik NA, Ali A, Patel R (2013) Role of 1-methyl-3-octyl imidazolium chloride in the micellization behavior of amphiphilic drug amitriptyline hydrochloride. Colloids Surf B Biointerfaces 112:460–465
33. Ohno H (2011) Electrochemical aspects of ionic liquids. John Wiley & Sons Inc, New Jersey
34. Jana S, Parthiban A, Chai CLL (2010) Transparent, flexible and highly conductive ion gels from ionic liquid compatible cyclic carbonate network. Chem Commun 46:1488–1490
35. Zhao Y, Yue X, Wang X, Huang D, Chen X (2012) Micelle formation by N-alkyl-N-methylpiperidinium bromide ionic liquids in aqueous solution. Colloids Surf A Physicochem Eng Asp 412:90–95
36. Wei Y, Wang F, Zhang Z, Ren C, Lin Y (2014) Micellization and thermodynamic study of 1-Alkyl-3-methylimidazolium tetrafluoroborate ionic liquids in aqueous solution. J Chem Eng Data 59:1120–1129
37. Marrucho IM, Branco LC, Rebelo LPN (2014) Ionic liquids in pharmaceutical applications. Annu Rev Chem Biomol Eng 5:527–546
38. Geng F, Zheng L, Yu L, Li G, Tung C (2010) Interaction of bovine serum albumin and long-chain imidazolium ionic liquid measured by fluorescence spectra and surface tension. Process Biochem 45:306–311
39. Hua Y, Junyong W, Guoliang D, Aiguo Z, Hao C, Jianguo Y, Denan H (2012) Interaction mechanisms of ionic liquids [Cnmim]Br (n=4, 6, 8, 10) with bovine serum albumin. J Lumin 132:622–628
40. Mahajan S, Sharma R, Mahajan RK (2012) An investigation of drug binding ability of a surface active ionic liquid: micellization, electrochemical, and spectroscopic studies. Langmuir 28:17238–17246
41. Rao KS, Singh T, Trivedi TJ, Kumar A (2011) Aggregation behavior of amino acid ionic liquid surfactants in aqueous media. J Phys Chem 115:13847–13853
42. Pal A, Pillania A (2014) Self-aggregation of ionic liquid 1-butyl-2,3-imethylimidazolium tetrafluoroborate [C_4mmim][BF_4] in

aqueous media: a conductometric, volumetric and spectroscopic study. Thermochim Acta 597:41–47
43. Wang X, Yu L, Jiao J, Zhang H, Wang R, Chen H (2012) Aggregation behavior of COOH-functionalized imidazolium-based surface active ionic liquids in aqueous solution. J Mol Liq 173: 103–107
44. Kamboj R, Bharmoria P, Chauhan V, Singh S, Kumar A, Mithu VS, Kang TS (2014) Micellization behavior of morpholinium-based amide-functionalized ionic liquids in aqueous media. Langmuir 30:9920–9930
45. Dong B, Gao Y, Su Y, Zheng L, Xu J, Inoue T (2010) Self- aggregation behavior of fluorescent carbazole-tailed imidazolium ionic liquids in aqueous solutions. J Phys Chem B 114:340–348
46. Shi L, Li N, Yan H, Gao Y, Zheng L (2011) Aggregation behavior of long-chain n-aryl imidazolium bromide in aqueous solution. Langmuir 27:1618–1625
47. Garcia MT, Ribosa I, Perez L, Manresa A, Comelles F (2013) Aggregation behavior and antimicrobial activity of ester-functionalized imidazolium and pyridinium-based ionic liquids in aqueous solution. Langmuir 29:2536–2545
48. Bordes R, Tropsch J, Holmberg K (2010) Role of an amide bond for self-assembly of surfactants. Langmuir 26:3077–3083
49. Zhang ZQ, Xu FG, Tai S, Liu X, Mo S, Niu F (2012) Surface tension and aggregation properties of novel cationic gemini surfactants with diethyl ammonium head groups and a diamido spacer. Langmuir 28:11979–11987
50. Hoque J, Kumar P, Aswal VK, Haldar V (2012) Aggregation properties of amide bearing cleavable gemini surfactants by small angle neutron scattering and conductivity studies. J Phys Chem B 116: 9718–9726
51. Hansen GE, Dennison MD (1952) The potential constants of ethane. J Chem Phys 20:313–326
52. Allen HC Jr, Plyler EK (1958) The structure of ethylene from infrared spectra. J Am Chem Soc 80:2673–2676
53. Mannhold R, Rekker RF, Dross K, Bijlo G, De Vries G (1998) The lipophilic behaviour of organic compounds. 1. An updating of the hydrophobic fragmental constant approach. Quant Struct Act Relat 17:517–536
54. Klevens HB (1953) Structure and aggregation in dilate solution of surface active agents. J Am Oil Chem Soc 30:74–80
55. Durairaj B, Blum FD (1985) Micelle formation and terminal double bonds in sodium carboxylates. J Colloid Interface Sci 106:561–564
56. Sprague ED, Duecker DC, Larrabee CE (1983) The effect of a terminal double bond on the micellization of a simple ionic surfactant. J Colloid Interface Sci 92:416–421
57. Larrabee CE, Sprague ED (1986) Aggregation of sodium undecanoate and sodium 10-undecenoate in water at 37°C: Vapor pressure osmometry. J Colloid Interface Sci 114:256–260
58. Damas C, Vannier L, Arabri M, Duchene A, Coudert R (1998) Micellar properties of a new series of stereochemical sodium carboxylates bearing double bonds near their ionic heads in aqueous media. J Colloid Interface Sci 198:323–329
59. Damas C, Vannier L, Naejus R, Coudert R (1999) Influence of structural modifications near the polar head of sodium carboxylates on their aqueous solution behavior. Colloids Surf A Physicochem Eng Asp 152:183–187
60. Yokoyama S, Nakagaki M (1993) Effect of double bond on the surface properties of aqueous solutions of eicosapolyenoic acids. Colloid Polym Sci 271:512–518
61. Kuiper JM, Buwalda RT, Hulst R, Engberts JBFN (2001) Novel pyridinium surfactants with unsaturated alkyl chains: aggregation behavior and interactions with methyl orange in aqueous solution. Langmuir 17:5216–5224
62. Lucero DG, Xometl OO, Palou RM, Likhanova NV, Aguilar MAD, Febles VG (2011) Synthesis of selected vinylimidazolium ionic liquids and their effectiveness as corrosion inhibitors for carbon steel in aqueous sulfuric acid. Ind Eng Chem Res 50:7129–7140
63. Luo SC, Sun S, Deorukhkar AR, Lu JT, Bhattacharyya A, Lin IJB (2011) Ionic liquids and ionic liquid crystals of vinyl functionalized imidazolium salts. J Mater Chem 21:1866–1873
64. Crescenzo AD, Demurtas D, Renzetti A, Siani G, Maria PD, Meneghetti M, Prato M, Fontana A (2009) Disaggregation of single-walled carbon nanotubes (SWNTs) promoted by the ionic liquid-based surfactant 1-hexadecyl-3-vinyl-imidazolium bromide in aqueous solution. Soft Matter 5:62–66
65. Crescenzo AD, Aschi M, Canto ED, Giordani S, Demurtas D, Fontana A (2011) Structural modifications of ionic liquid surfactants for improving the water dispersibility of carbon nanotubes: an experimental and theoretical study. Phys Chem Chem Phys 13: 11373–11383
66. Damas C, Brembilla A, Baros F, Viriot ML, Lochon P (1994) Synthesis and behaviour study of amphiphilic polyvinylimidazolium salts in aqueous media: Effects of the microdomains on a bimolecular reaction involving hydrophobic reactants. Eur Polym J 30:1215–1222
67. Damas C, Baggio S, Brembilla A, Lochon P (1997) Microstructure study of new amphiphilic copolymers from 3-alkyl-1-vinylimidazolium salts. Eur Polym J 33:1219–1224
68. Harkins WD, Jordan HF (1930) A method for the determination of surface and interfacial tension from the maximum pull on a ring. J Am Chem Soc 52:1751–1772
69. Rosen MJ (2004) Surfactants and Interfacial Phenomena, 3rd edn. John Wiley & Sons, New Jersey
70. Zana R (1980) Ionization of cationic micelles: effect of the detergent structure. J Colloid Interface Sci 78:330–337
71. McAuliffe C (1966) Solubility in water of paraffin, cycloparaffin, olefin, acetylene, cycloolefin, and aromatic hydrocarbons. J Phys Chem 70:1267–1275
72. Tanford C (1980) The hydrophobic effect: formation of micelles and biological membranes. John Wiley, New York
73. Ray GB, Chakraborty I, Ghosh S, Moulik SP, Palepu R (2005) Self-aggregation of alkyltrimethylammonium bromides (C_{10}-, C_{12}-, C_{14}-, and C_{16}TAB) and their binary mixtures in aqueous medium: a critical and comprehensive assessment of interfacial behavior and bulk properties with reference to two types of micelle formation. Langmuir 21:10958–10967
74. Mukerjee P (1967) Nature of the association equilibriums and hydrophobic bonding in aqueous solutions of association colloids. Adv Colloid Interf Sci 1:242–275
75. Mukerjee P, Mysels, KJ (1972) Critical Micelle Concentrations of Aqueous Surfactant Systems. National Bureau of Standards of NSRDS-NBS 36, Washington, DC 20234.
76. Mosquera V, Rio JM, Attwood D, Garcia M, Jones MN, Prieto G, Suarez MJ, Sarmiento F (1998) A Study of the aggregation behavior of hexyltrimethylammonium bromide in aqueous solution. J Colloid Interface Sci 206:66–76
77. Bashford MT, Woolley EM (1985) Enthalpies of dilution of aqueous decyl-, dodecyl-, tetradecyl-, and hexadecyltrimethylammonium bromides at 10, 25, 40, and 55 °C. J Phys Chem 89:3173–3179
78. Stauff J (1983) Z Phys Chem A 183:55
79. Klevens HB (1952) Solubilization in alcohol—soap micelles II electrolytes as additives. J Am Chem Soc 74:4624–4626
80. Hafiane A, Dhahbi M, Chasseray X, Lemordant DJ (1998) J Colloid Interface Sci 205:21–25
81. Zhao Y, Gao S, Wang J, Tang J (2008) Aggregation of Ionic Liquids C_nMeImBr (n) 4, 6, 8, 10, 12) in D2O: a NMR study. J Phys Chem B 112:2031–2039
82. Baker GA, Pandey S, Pandey S, Baker S (2004) A new class of cationic surfactants inspired by *N*-alkyl-*N*-methyl pyrrolidinium ionic liquids. Analyst 129:890–892

83. Jones MJ, Chapman D (1995) Micelles, monolayers, and biomembranes. Wiley-LISS, New York
84. Holmberg K, Jonsson B, Kronberg B, Lindman B (2003) Surfactants and Polymers in aqueous solution. John Wiley & Sons Ltd, New York
85. Tadros TF (2005) Applied Surfactants, Principles and Applications . Wiley-VCH Verlag GmbH & Co, KGaA-Weinheim
86. Nusselder JJH, Engberts JBFN (1992) Toward a better understanding of the driving force for micelle formation and micellar growth. J Colloid Interface Sci 148:353–361
87. Sirieix-Plenet J, Gaillon L, Letellier P (2004) Behaviour of a binary solvent mixture constituted by an amphiphilic ionic liquid, 1-decyl-3-methylimidazolium bromide and water: Potentiometric and conductimetric studies. Talanta 63:979–986
88. Turro NJ, Yekta A (1978) Luminescent probes for detergent solutions. A simple procedure for determination of the mean aggregation number of micelles. J Am Chem Soc 100:5951–5952
89. Dong DC, Winnik MA (1982) Photochem. The Py scale of solvent polarities. Solvent effects on the vibronic fine structure of pyrene fluorescence and empirical correlations with ET and Y values. Photobiol 35:17–21
90. Wang GJ, Engberts JBFN (1994) Induction of aggregate formation of cationic polysoaps and surfactants by low concentrations of additives in aqueous solution. Langmuir 10:2583–2587
91. Quadrifoglio F, Crescenzi V (1971) The interaction of methyl orange and other azo-dyes with polyelectrolytes and with colloidal electrolytes in dilute aqueous solution. J Colloid Interface Sci 35: 447–459
92. Dutta RK, Bhat SN (1993) interaction of methyl orange with submicellar cationic surfactants. Bull Chem Soc Jpn 66:2457–2460
93. Dutta RK, Bhat SN (1996) Interaction of phenazinium dyes and methyl orange with micelles of various charge types. Colloids Surf A Physicochem Eng Asp 106:127–134
94. Buwalda RT, Jonker JM, Engberts JBFN (1999) Aggregation of azo dyes with cationic amphiphiles at low concentrations in aqueous solution. Langmuir 15:1083–1089
95. Karukstis KK, Savin DA, Loftus CT, Angelo NDD (1998) Spectroscopic studies of the interaction of methyl orange with cationic alkyltrimethylammonium bromide surfactants. J Colloid Interface Sci 203:157–163
96. Lueck HB, Rice BL, McHale JL (1992) Aggregation of triphenylmethane dyes in aqueous solution: Dimerization and trimerization of crystal violet and ethyl violet. Spectrochim Acta A 48:819–828
97. Lueck HB, Mchale JL, Edwards WD (1992) Symmetry-breaking solvent effects on the electronic structure and spectra of a series of triphenylmethane dyes. J Am Chem Soc 114:2342–2348